Electron spin contrast of Purcell-enhanced nitrogen-vacancy ensembles in nanodiamonds

Electron spin contrast of Purcell-enhanced nitrogen-vacancy ensembles in nanodiamonds

S. Bogdanov,[1,2,*] M. Y. Shalaginov,[1,2] A. Akimov,[3,4,5] A. S. Lagutchev,[2] P. Kapitanova,[6] J. Liu,[7] D. Woods,[1,2] M. Ferrera,[8] P. Belov,[6] J. Irudayaraj,[7] A. Boltasseva,[1,2] and V. M. Shalaev[1,2,3]

[1]*School of Electrical and Computer Engineering, Purdue Quantum Center, Purdue University, West Lafayette, Indiana 47907, USA*

[2]*Birck Nanotechnology Center, Purdue University, West Lafayette, Indiana 47907, USA*

[3]*Department of Physics and Astronomy, Texas A&M University, College Station, Texas 77843, USA*

[4]*Russian Quantum Center, ulica Novaya 100, BC "Ural," Skolkovo Innovation Center, Moscow Region 143025, Russia*

[5]*Lebedev Physical Institute, RAS, Leninskij prospekt 53, Moscow 119991, Russia*

[6]*The International Research Centre for Nanophotonics and Metamaterials, ITMO University, Saint Petersburg 197101, Russia*

[7]*Agricultural and Biological Engineering, Purdue University, West Lafayette, Indiana 47907, USA*

[8]*Institute of Photonics and Quantum Sciences, SUPA, Heriot-Watt University, EH14 4AS Edinburgh, United Kingdom*

(Received 21 March 2017; revised manuscript received 7 June 2017; published 25 July 2017)

Nitrogen-vacancy centers in diamond allow for coherent spin-state manipulation at room temperature, which could bring dramatic advances to nanoscale sensing and quantum information technology. We introduce a method for the optical measurement of the spin contrast in dense nitrogen-vacancy (NV) ensembles. This method brings insight into the interplay between the spin contrast and fluorescence lifetime. We show that for improving the spin readout sensitivity in NV ensembles, one should aim at modifying the far-field radiation pattern rather than enhancing the emission rate.

DOI: 10.1103/PhysRevB.96.035146

I. INTRODUCTION

Nitrogen-vacancy color centers (NVs) in diamond are fluorescent lattice defects resulting from a vacancy and an adjacent nitrogen substitution [1,2]. These color centers have proven to be excellent test beds for novel nanoscale optical devices. Ultrasensitive electromagnetic field [3–8], strain [9,10], pressure [11], and temperature [12,13] sensors as well as integrated quantum information processors [14–16] operating at ambient conditions have been prototyped using NVs. These capabilities are in large part due to the unique properties of the NV's electron spin, which may be optically initialized and manipulated by microwave signals [17,18]. The NV exhibits a spin-dependent fluorescence rate, which can be used for optical spin-state readout [19]. The relative difference between the fluorescence rates emitted by the $m_s = 0$ and $m_s = \pm 1$ states (where m_s is a spin projection) is commonly called the spin contrast. This spin contrast constitutes the readout signal for spin-based qubits and sensors. Numerous potential applications of NVs such as nanoscale magnetometry and quantum information processing demand the optimization of the spin readout. Such optimization should take into account both the overall photon detection rate and the magnitude of the spin contrast.

The observed fluorescence intensity is typically limited by the inefficiency of photon collection. To combat this inefficiency, various photonic and plasmonic approaches have been tried such as solid immersion lenses [20–22], photonic nanowires [23], cavities [24–28], plasmonic apertures [29], nanoantennas [30,31], waveguides [32–34], and metamaterials [35]. These structures work by modifying the near-field and far-field behavior of the emission, thus drastically enhancing the collection efficiency. Additionally, when optically coupled to a photonic resonator and/or a plasmonic structure, the NV center exhibits a reduction of fluorescence lifetime. This reduction is called the Purcell effect and results from a high local photonic density of states (PDOS) [36]. This effect can further improve photon detection rates. However, despite the vast knowledge accumulated about the NV level dynamics [1], the effect of the fluorescence lifetime on the spin contrast remains unclear. The dependence of spin contrast on fluorescence lifetime has been investigated theoretically using different models [37,38]. Here, we present the first experimental study that quantitatively explores this dependence.

The spin contrast in single NV centers monotonically increases with the optical excitation rate, and therefore, it is usually advantageous to operate isolated NV centers in the optical saturation regime. However, for sensing applications such as magnetometry, one often chooses to employ NV ensembles (NVEs) with interdefect separation distances (IDSDs) on the order of 10 nm and smaller [39–42], yielding high levels of fluorescence. Unlike single NV centers, these ensembles must be operated at optical excitation rates well below the saturation level because the spin contrast exhibits an optimum well before the saturation regime is reached. This observation is confirmed by unpublished measurements conducted by other groups [43]. In this work, we measure the dependence of the spin contrast on the fluorescence lifetime in dense NV ensembles (IDSD ≈ 8 nm). We also explore the implications of this dependence for the design of NV-based nanophotonic devices. For this study, we introduce a technique for spin-contrast measurement that is particularly suited for such NVEs.

II. EXPERIMENTAL TECHNIQUES

A. Sample fabrication

Individual nanodiamonds (76 ± 20 nm in size), each containing an NVE (400 NV centers, on average), were dispersed on a sapphire substrate. In order to create a wide distribution of fluorescence lifetimes,

*sbogdan@purdue.edu

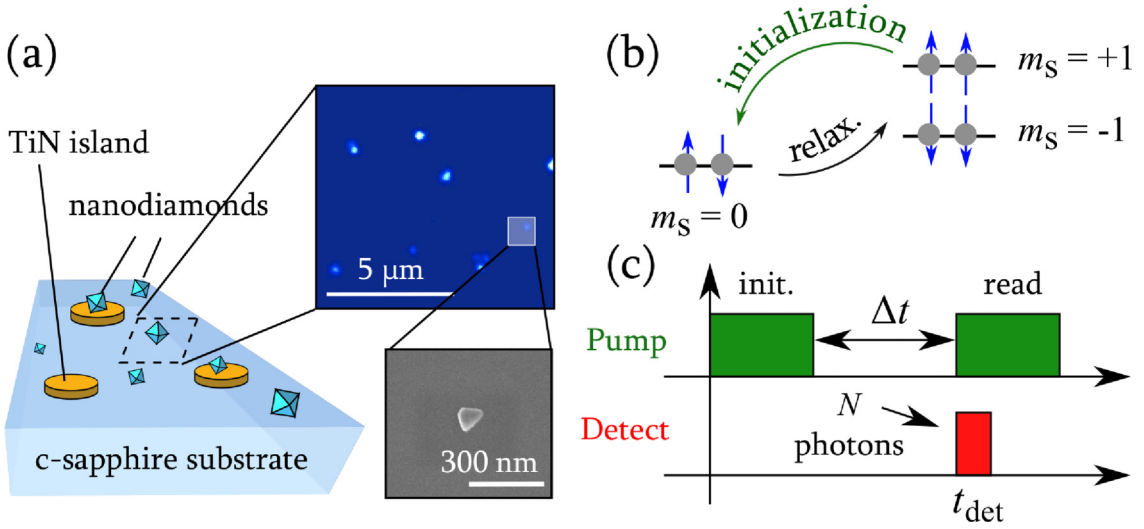

FIG. 1. (a) Sample layout: islands of plasmonic TiN (200 nm thick and 500 μm in diameter) and dispersed nanodiamonds with NV center ensembles (NVEs) on a *c*-sapphire substrate. Blowups show a fluorescence map of NVEs and an SEM image of a typical nanodiamond used in the study. (b) Ground-state spin-level diagram showing the processes of optical initialization and subsequent thermal relaxation. (c) Spin-contrast measurement scheme. The number of photons registered during the detection window of duration t_{det} depends on the degree of spin relaxation occurring during the time Δt.

0.5-mm-diameter plasmonic titanium nitride (TiN) [44] islands were formed on the substrate. The NVEs experienced different PDOS depending on their location. Higher PDOS at the surface of TiN islands is expected due to confined surface plasmon-polariton (SPP) modes [45]. An average lifetime shortening of about 3 times is expected for NVEs on TiN compared to those on sapphire substrate from simulations of total power emitted by a dipole in the center of a 76-nm nanodiamond, assuming unity quantum yield. The distribution of the observed lifetime decrease is due to variations in both nanodiamond size and NVE quantum yield. More details on the contribution of the SPP modes to the fluorescence lifetime can be found in the Supplemental Material [46]. Figure 1(a) shows the layout of the sample and probed areas. We chose an area on sapphire and an area on a TiN island, randomly selected approximately ten nanodiamonds from each area, and measured their fluorescence lifetimes and spin-contrast values.

B. Spin contrast measurement

To reduce the number of experimental uncertainties affecting the measurement of the spin contrast, we have devised a method based on the process of thermal spin relaxation. First, an initializing optical pulse [see Fig. 1(c)] projects the spin into a state with a predominantly $m_s = 0$ projection. After a controlled time delay Δt, part of the population relaxes back to the $m_s = \pm 1$ states [see Fig. 1(b)]. Finally, the "read" pulse is applied, and the fluorescence is collected during the first $t_{det} =$ 300 ns of the read pulse [see Fig. 1(c)]. The delay Δt is varied to produce different spin populations, starting from a predominantly (70% to 90% [47–49]) $m_s = 0$ spin and ending with a thermally relaxed spin (1/3 of the population in the $m_s = 0$ state). As Δt surpasses the spin-relaxation time T_1, the contrast between the relaxed spin and the initialized spin asymptotically reaches a constant value corresponding to a complete thermal spin relaxation. We refer to this limit value as the T_1 spin contrast: $C_{T1} = (N_\infty - N_0)/N_0$. Here, N_0 and N_∞ are the numbers of detected photons in the cases of initialized spin and a fully thermalized spin, respectively. Typical spin-relaxation curves for NVEs on sapphire and on TiN are shown in Fig. 2(a), featuring spin-relaxation times in the 100-μs range.

Unlike a conventional spin-contrast measurement based on coherent spin population inversion [50], this technique is advantageous for large NVEs. A resonant microwave pulse would address only a group of NV centers forming the same angle with the axis of the dc magnetic field. In contrast, thermal relaxation equally affects all the NV centers in the ensemble, leading to 1/3 of the whole spin population residing in the $m_s = 0$ state. C_{T1} measured on an NVE represents 2/3 of the spin contrast

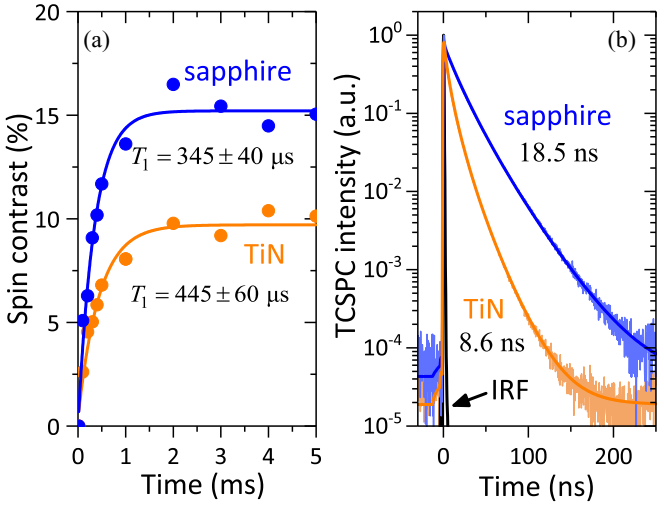

FIG. 2. (a) Typical spin-relaxation and (b) fluorescence decay curves for NVEs found on sapphire (blue) and TiN (orange). The spin contrast is measured as a normalized difference between the fluorescence signals of partially thermalized spins and optically initialized spins.

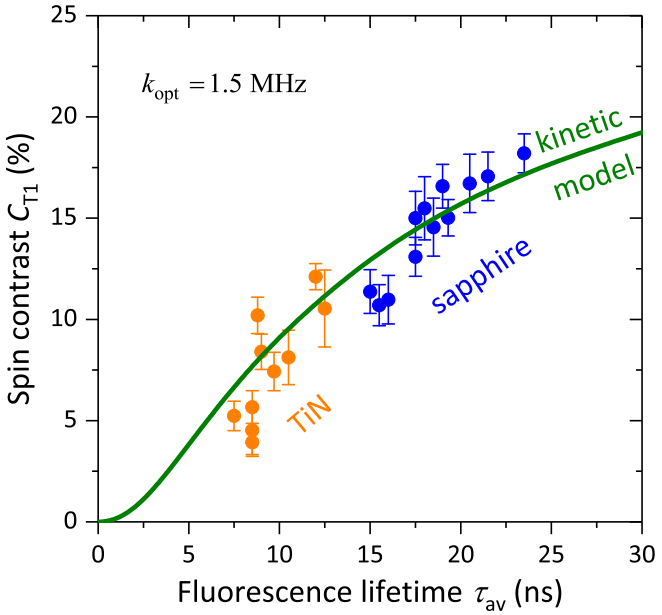

FIG. 3. Spin decay contrast C_{T1} values for NVEs with different lifetimes measured for an optical excitation rate of approximately 1.5 MHz. The trend agrees well with the results of the simulation based on a kinetic model of the NV.

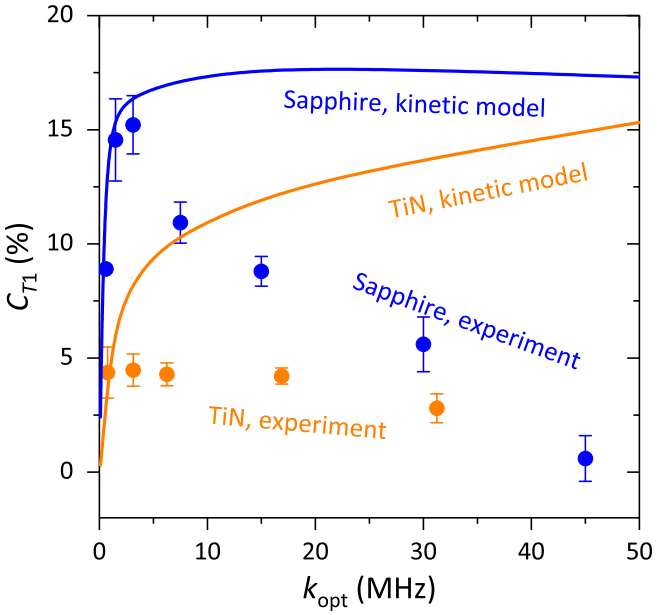

FIG. 4. Dependences of C_{T1} on optical power for NVEs on sapphire and TiN show a decrease at strong excitation rates. Solid lines are obtained from the five-level kinetic model of the NV center.

C_π obtained from Rabi oscillations of a single NV center. The measurement of C_{T1} is not affected by strong spin decoherence rates present in dense ensembles. Finally, it does not require the application of dc and ac magnetic fields and therefore is not affected by their temporal and spatial variations. The present method for quantifying the contrast constitutes a way to evaluate the suitability of the given NV ensemble for sensing and other relevant applications. However, in an actual sensing experiment, ac and dc magnetic fields will be required.

C. Fluorescence lifetime measurement

The fluorescence lifetime measurements were performed using the time-correlated single-photon counting (TCSPC) technique [51]. The fluorescence decay curves for NVEs on sapphire and on TiN are shown in Fig. 2(b). The fluorescence decay data are fitted by sums of exponential decays for ensembles of two-level systems, assuming that their lifetimes are Γ distributed [46].

III. EXPERIMENTAL RESULTS

We correlated the fluorescence lifetimes and spin contrasts for a collection of NVEs found on the sapphire and TiN areas (see Fig. 3). The range of fluorescence lifetimes for NVEs found on sapphire spans 15 to 24 ns. This spread of lifetimes can be attributed to several effects. For example, variations of the local density of states experienced by different NVEs [52,53] due to variations in nanocrystal sizes and shapes as well as varying direct nonradiative decay rates [54] can affect the observed ensemble lifetimes. The TiN film's SPP modes [55] contribute to the local PDOS [46] and increase the radiative rates of the NVEs [35]. Correspondingly, the lifetimes measured on TiN area range from 7.5 to 12.5 ns. We have found that the spin contrast strongly depends on the fluorescence lifetime, with values of spin contrast C_{T1} dropping to below 5% for the NVEs with the shortest lifetimes.

The laser power was calibrated to ensure that both NVEs on sapphire and TiN experience a similar optical excitation rate $k_{opt} \approx 1.5$ MHz. The pump laser power P_l can be converted to the excitation rate k_{opt} using a proportionality constant $c_{opt} = k_{opt}/P_l$, which is substrate dependent. The constant c_{opt} can be retrieved by fitting NVE fluorescence saturation curves. More details on the calibration of the excitation rate can be found in the Supplemental Material [46]. For excitation rates significantly exceeding 1.5 MHz, we found that the contrast C_{T1} drops and almost completely vanishes in strong saturation (Fig. 4) [46]. A small decrease in spin contrast is expected at high excitation rates from the simple kinetic model described below. As the spin initialization starts to occur faster than the duration of the detection window, the fluorescence from the remainder of the detection window becomes identical for the two spin subsystems, thus reducing the spin contrast. Additionally, two-photon-induced ionization becomes significant at powers beyond optical saturation, leading to the loss of spin information and of spin contrast. However, the observed decrease of C_{T1} with laser power is much steeper than the kinetic theory predicts. It is also stronger than what is expected from the ionization of individual NV centers. The origin of this drop in spin contrast is still under investigation. Optically detected magnetic resonance spectra of our NVEs show high levels of strain, possibly caused by high impurity concentration [46]. The strong contrast decrease at high excitation rates could be attributed to the charge exchange processes involving proximal NV centers and/or nitrogen impurities. Such dynamics may be especially pronounced in dense ensembles like ours, e.g., due to Auger-type effects. This effect makes it impractical to work in the saturation regime and

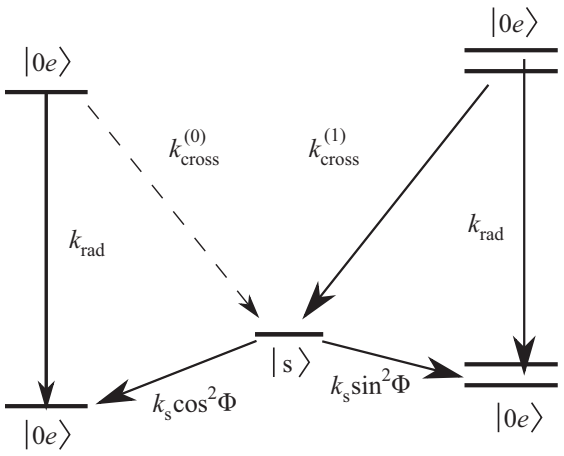

FIG. 5. A simplified representation of the NV center's energy levels and transition rates. The two levels on the left (right) are the excited and ground triplet states of the $m_s = 0(\pm 1)$ subsystem. The level s in the middle is the metastable spin-singlet level.

limits the observable spin-contrast values. However, our results and those observed in other groups [43] suggest that such spin-contrast behavior is a general phenomenon associated with dense ensembles, rather than an accidental observation.

IV. KINETIC MODELING OF THE SPIN CONTRAST

A. Qualitative discussion

Before rigorously investigating the observed dependence of spin contrast on fluorescence lifetime, we present a qualitative explanation based on the NV level structure (see Fig. 5). For simplicity, in this discussion we assume that the optical excitation rate is much lower than all the level decay rates. Following the absorption of a photon, both the excited state (ES) and the singlet levels relax into the ground-state (GS) levels before the next photon is absorbed. The ESs of the $m_s = 0$ and $m_s = \pm 1$ subsystems (i.e., levels $|0e\rangle$ and $|1e\rangle$, respectively) have equal radiative decay rates k_{rad} into their respective GSs $|0g\rangle$ and $|1g\rangle$. However, the fluorescence rate of the $m_s = 0$ subsystem is higher because the nonradiative decay of $|0e\rangle$ through the singlet state $|s\rangle$ is less probable than that of $|1e\rangle$ ($k_{\text{cross}}^{(0)} < k_{\text{cross}}^{(1)}$). Under an optical pulse, two NV centers initially prepared in $m_s = 0$ and $m_s = \pm 1$ states will exhibit different levels of fluorescence, leading to a spin contrast. The decay $|1e\rangle \rightarrow |s\rangle \rightarrow |0g\rangle$ through the singlet state is a nonradiative process (intersystem crossing), and its rates k_{cross} and k_s are not sensitive to the PDOS. Shortening the direct decay lifetime leads to a smaller relative probability of the nonradiative decay and therefore a reduced spin contrast [37]. Hence, for the case of a low excitation rate, one indeed expects to measure smaller spin contrasts in a higher PDOS environment, as illustrated by our data.

B. Numerical modeling

The theoretical simulation of the observed dependence requires a careful analysis of the transient populations of the NV under an optical pulse. The evolution of NV level populations with time can be derived from the master equation $\dot{\mathbf{m}} = \mathbf{A}\mathbf{m}$ [57] that governs the kinetics of the NV center transitions. In this equation, $\mathbf{m}^T = [\rho_{0g}\rho_{1g}\rho_s\rho_{0e}\rho_{1e}]$ is the unknown vector consisting of level populations. The matrix $\mathbf{A}$ is given by

$$\mathbf{A} = \begin{bmatrix} -k_{\text{opt}} & 0 & k_s\cos^2\Phi & k_{\text{rad}} & 0 \\ 0 & -k_{\text{opt}} & k_s\sin^2\Phi & 0 & k_{\text{rad}} \\ 0 & 0 & -k_s & k_{\text{cross}}^{(0)} & k_{\text{cross}}^{(1)} \\ k_{\text{opt}} & 0 & 0 & -k_{\text{rad}} - k_{\text{cross}}^{(0)} & 0 \\ 0 & k_{\text{opt}} & 0 & 0 & -k_{\text{rad}} - k_{\text{cross}}^{(1)} \end{bmatrix}. \quad (1)$$

Here, $k_{\text{rad}} = \tau_{\text{rad}}^{-1}$ is the rate of spin-conserving direct ES decay, k_{opt} is the optical pumping rate, $k_{\text{cross}}^{(i)}$ are the intersystem crossing rates from $|0e\rangle$ and $|1e\rangle$ to the singlet state, k_s is the deshelving rate of the singlet state, and the angle Φ quantifies the branching ratio of the singlet-state decay. We assume that the spin decay is negligible during the optical pulse duration of 15 μs, which is well supported by the spin-relaxation curves on Fig. 2(a). The number of photons arriving within the detection window t_{det} is $N = \int_0^{t_{\text{det}}} k_{\text{rad}}[\rho_{0e}(t) + \rho_{1e}(t)]dt$. Many NV centers are present in each NVE, and the nanocrystal lattice orientations are random. Consequently, the calculated photon numbers are obtained by integrating the fluorescence rates over the NV axis directions and lifetimes. The distribution of NV axis directions is assumed to be isotropic, and the lifetimes are assumed to follow the Γ distribution [46]. We fitted the values of the kinetic parameters, starting from the numbers measured in a recent experiment [56]. We found good agreement with our data by adjusting only the spin-dependent nonradiative intersystem crossing rates $k_{\text{cross}}^{(i)}$ from ES to the singlet state. These parameters were fitted as $k_{\text{cross}}^{(0)} = 5 \pm 2$ MHz and $k_{\text{cross}}^{(1)} = 30 \pm 4$ MHz, agreeing fairly well with values found in other experiments [57,58]. The deshelving rate of the singlet state ($k_s = 7$ MHz) and the branching angle of the singlet decay ($\Phi = 33°$) were left unchanged. The radiative ES decay rate k_{rad} depends on the local environment of each NVE and is determined from TCSPC measurements.

At optical excitation rates, exceeding 1.5 MHz, we observe a deviation of the spin contrast from this kinetic model [46]. In all spin-contrast measurements from Fig. 3 the laser powers were such that this deviation was negligible. Using the above parameters, a reasonably good agreement with the experiment was reached within the entire range of measured lifetimes (7 to 24 ns), as seen from Fig. 3.

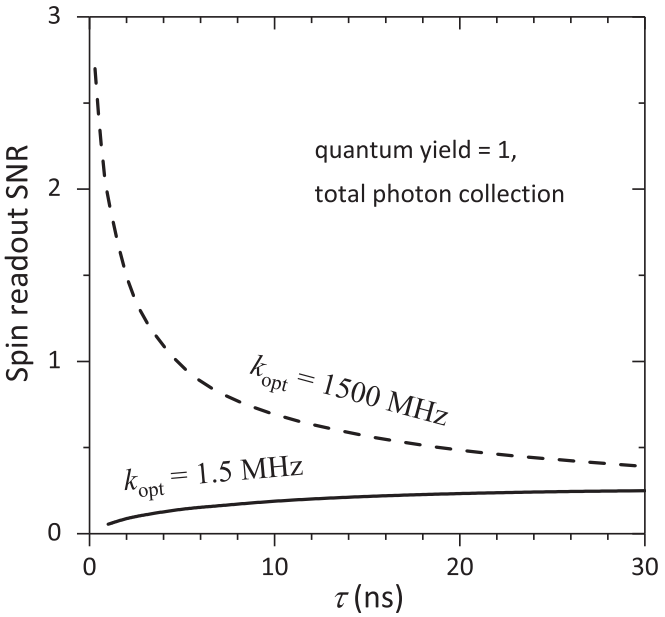

FIG. 6. Calculated electron spin readout signal-to-noise ratio for a single NV, under weak and strong optical excitation rates, assuming optimal durations of detection window t_{det}. Dashed line: single-shot signal-to-noise ratio as a function of the total fluorescence lifetime, assuming unity quantum yield and total collection of fluorescence, $k_{opt} = 1500$ MHz (deep saturation). Solid line: single-shot signal-to-noise ratio assuming optical excitation rate of $k_{opt} = 1.5$ MHz, used in our experiment.

V. DISCUSSION

Our data show that the shortening of fluorescence lifetime in NVEs results in a decrease of the optical spin contrast at low excitation rates. This in turn affects the electron spin readout sensitivity. The single-shot spin readout signal-to-noise (SN) ratio can be assessed as being $\approx C\sqrt{N_0/(2-C)}$. Here, C is the spin contrast, and N_0 is the number of photons collected within the detection window for an NV center initialized in the $m_s = 0$ state. Figure 6 presents SN ratio plots calculated from the kinetic model above. Plasmonic or resonant photonic structures, such as nanoantennas and nanocavities, can increase N_0 by improving the apparent quantum yield and collection efficiency thanks to a high PDOS in specific modes. Nevertheless, at low pump powers, the rapid drop in contrast for NV centers with lifetimes below 5 ns represents a serious limitation to the SN ratio (solid line in Fig. 6). Thus, the spin readout improvement for NV ensembles operating below optical saturation would be best achieved by methods that avoid significant shortening of the fluorescence lifetime. For example, solid immersion lenses [20], bull's-eye gratings [59], photonic nanowires [23], and bulk diamond waveguides [27,60] lead to high collection efficiency through the modification of the far-field radiation pattern, without creating a high PDOS in any particular mode.

The negative effect of the lifetime shortening on the spin readout SN ratio in dense NVEs is due to the fact that these NVEs must be operated at low optical excitation rates. In our model, we can remove this limitation by considering the dynamics of a single NV, unaffected by the ensemble effects. In particular, the kinetic model is expected to still hold true at saturating optical powers [56]. In this regime, the spin contrast depends only on the nonradiative transition rates k_s and $k_{cross}^{(i)}$ and therefore should not depend on the fluorescence lifetime. Consequently, at $k_{opt} = 1500$ MHz, the Purcell effect could improve the spin readout SN ratio significantly (see dashed line in Fig. 6), even starting with perfect photon collection. This implies that Purcell-effect-based collection schemes could be efficiently utilized in diamond crystals with low defect concentration. We note, however, that these results may be affected by the presence of direct spin-nonconserving ES-GS transitions [37,46].

VI. SUMMARY AND CONCLUSIONS

We have studied the dependence of the spin contrast in nanodiamond-based NVEs as a function of their fluorescence lifetime. Lifetimes up to 24 ns were observed for NVEs in a dielectric environment and as short as 7 ns for NVEs in a plasmonic environment, with the corresponding spin contrast C_{T1} values ranging from 18% to 4%. We have developed a method for measuring the optical spin contrast in NV ensembles, relying on thermal spin relaxation and involving no microwave and static magnetic fields. The experimentally obtained dependence of the spin contrast on the lifetime can be adequately described by using a linear rate-equation-based model. Our results can be used to optimize the spin readout sensitivity of NVEs in various photon collection schemes and pave the way for improved sensing schemes utilizing NVEs.

ACKNOWLEDGMENTS

The authors thank M. D. Lukin, A. Safira, A. Sipahigil, R. Landig, J. Choi, D. Hopper, and L. Bassett for helpful discussions, S. Peana and C. Devault for their assistance with manuscript preparation, and D. Peroulis for providing the microwave testing equipment for preliminary tests. This work was partially supported by AFOSR-MURI Grant No. FA9550-12-10024, ONR-DURIP Grant No. N00014-16-1-2767, and NSF Grants No. MRSEC DMR-1120923 and No. META-PREM DMR-1205457. A.A. acknowledges the Russian Foundation for Basic Research Grant No. 14-29-07127.

[1] M. W. Doherty, N. B. Manson, P. Delaney, F. Jelezko, J. Wrachtrup, and L. C. L. Hollenberg, Phys. Rep. **528**, 1 (2013).
[2] A. Gruber, A. Dräbenstedt, C. Tietz, L. Fleury, J. Wrachtrup, and C. von Borczyskowski, Science **276**, 2012 (1997).
[3] L. Rondin, J.-P. Tetienne, T. Hingant, J.-F. Roch, P. Maletinsky, and V. Jacques, Rep. Prog. Phys. **77**, 056503 (2014).
[4] J. R. Maze, P. L. Stanwix, J. S. Hodges, S. Hong, J. M. Taylor, P. Cappellaro, L. Jiang, M. V. G. Dutt, E. Togan, A. S. Zibrov,

A. Yacoby, R. L. Walsworth, and M. D. Lukin, Nature (London) **455**, 644 (2008).
[5] G. Waldherr, J. Beck, P. Neumann, R. S. Said, M. Nitsche, M. L. Markham, D. J. Twitchen, J. Twamley, F. Jelezko, and J. Wrachtrup, Nat. Nanotechnol. **7**, 105 (2011).
[6] F. Dolde, H. Fedder, M. W. Doherty, T. Nöbauer, F. Rempp, G. Balasubramanian, T. Wolf, F. Reinhard, L. C. L. Hollenberg, F. Jelezko, and J. Wrachtrup, Nat. Phys. **7**, 459 (2011).
[7] H. Clevenson, M. E. Trusheim, C. Teale, T. Schröder, D. Braje, and D. Englund, Nat. Phys. **11**, 393 (2015).
[8] I. Lovchinsky, A. O. Sushkov, E. Urbach, N. P. de Leon, S. Choi, K. De Greve, R. Evans, R. Gertner, E. Bersin, C. Müller, L. McGuinness, F. Jelezko, R. L. Walsworth, H. Park, and M. D. Lukin, Science **351**, 836 (2016).
[9] M. E. Trusheim and D. Englund, New J. Phys. **18**, 123023 (2016).
[10] F. Grazioso, B. R. Patton, P. Delaney, M. L. Markham, D. J. Twitchen, and J. M. Smith, Appl. Phys. Lett. **103**, 101905 (2013).
[11] M. W. Doherty, V. V. Struzhkin, D. A. Simpson, L. P. McGuinness, Y. Meng, A. Stacey, T. J. Karle, R. J. Hemley, N. B. Manson, L. C. L. Hollenberg, and S. Prawer, Phys. Rev. Lett. **112**, 047601 (2014).
[12] G. Kucsko, P. C. Maurer, N. Y. Yao, M. Kubo, H. J. Noh, P. K. Lo, H. Park, and M. D. Lukin, Nature (London) **500**, 54 (2013).
[13] D. M. Toyli, C. F. D. Las Casas, D. J. Christle, V. V. Dobrovitski, and D. D. Awschalom, Proc. Natl. Acad. Sci. USA **110**, 8417 (2013).
[14] N. Y. Yao, L. Jiang, A. V. Gorshkov, P. C. Maurer, G. Giedke, J. I. Cirac, and M. D. Lukin, Nat. Commun. **3**, 15 (2010).
[15] T. van der Sar, Z. H. Wang, M. S. Blok, H. Bernien, T. H. Taminiau, D. M. Toyli, D. A. Lidar, D. D. Awschalom, R. Hanson, and V. V. Dobrovitski, Nature (London) **484**, 82 (2012).
[16] G. Waldherr, Y. Wang, S. Zaiser, M. Jamali, T. Schulte-Herbrüggen, H. Abe, T. Ohshima, J. Isoya, J. F. Du, P. Neumann, and J. Wrachtrup, Nature (London) **506**, 204 (2014).
[17] P. L. Stanwix, L. M. Pham, J. R. Maze, D. Le Sage, T. K. Yeung, P. Cappellaro, P. R. Hemmer, A. Yacoby, M. D. Lukin, and R. L. Walsworth, Phys. Rev. B **82**, 201201 (2010).
[18] N. Bar-Gill, L. M. Pham, A. Jarmola, D. Budker, and R. L. Walsworth, Nat. Commun. **4**, 1743 (2013).
[19] P. Neumann, J. Beck, M. Steiner, F. Rempp, H. Fedder, P. R. Hemmer, J. Wrachtrup, and F. Jelezko, Science **329**, 542 (2010).
[20] J. P. Hadden, J. P. Harrison, A. C. Stanley-Clarke, L. Marseglia, Y. L. D. Ho, B. R. Patton, J. L. O'Brien, and J. G. Rarity, Appl. Phys. Lett. **97**, 241901 (2010).
[21] T. Schröder, F. Gädeke, M. J. Banholzer, and O. Benson, New J. Phys. **13**, 055017 (2011).
[22] L. Marseglia, J. P. Hadden, A. C. Stanley-Clarke, J. P. Harrison, B. Patton, Y.-L. D. Ho, B. Naydenov, F. Jelezko, J. Meijer, P. R. Dolan, J. M. Smith, J. G. Rarity, and J. L. O'Brien, Appl. Phys. Lett. **98**, 133107 (2011).
[23] T. M. Babinec, B. J. M. Hausmann, M. Khan, Y. Zhang, J. R. Maze, P. R. Hemmer, and M. Loncar, Nat. Nanotechnol. **5**, 195 (2010).
[24] J. Wolters, G. Kewes, A. W. Schell, N. Nüsse, M. Schoengen, B. Löchel, T. Hanke, R. Bratschitsch, A. Leitenstorfer, T. Aichele, and O. Benson, Phys. Status Solidi B **249**, 918 (2012).
[25] A. Faraon, P. E. Barclay, C. Santori, K.-M. C. Fu, and R. G. Beausoleil, Nat. Photonics **5**, 301 (2011).
[26] J. Riedrich-Möller, S. Pezzagna, J. Meijer, C. Pauly, F. Mücklich, M. Markham, A. M. Edmonds, and C. Becher, Appl. Phys. Lett. **106**, 221103 (2015).
[27] M. J. Burek, Y. Chu, M. S. Z. Liddy, P. Patel, J. Rochman, S. Meesala, W. Hong, Q. Quan, M. D. Lukin, and M. Lončar, Nat. Commun. **5**, 5718 (2014).
[28] L. Li, T. Schröder, E. H. Chen, M. Walsh, I. Bayn, J. Goldstein, O. Gaathon, M. E. Trusheim, M. Lu, J. Mower, M. Cotlet, M. L. Markham, D. J. Twitchen, and D. Englund, Nat. Commun. **6**, 6173 (2015).
[29] J. T. Choy, B. J. M. Hausmann, T. M. Babinec, I. Bulu, M. Khan, P. Maletinsky, A. Yacoby, and M. Lončar, Nat. Photonics **5**, 738 (2011).
[30] S. Schietinger, M. Barth, T. Aichele, and O. Benson, Nano Lett. **9**, 1694 (2009).
[31] M. Geiselmann, R. Marty, J. Renger, F. J. García De Abajo, and R. Quidant, Nano Lett. **14**, 1520 (2014).
[32] D. E. Chang, A. S. Sorensen, P. R. Hemmer, and M. D. Lukin, Phys. Rev. B **76**, 035420 (2007).
[33] A. Huck, S. Kumar, A. Shakoor, and U. L. Andersen, Phys. Rev. Lett. **106**, 096801 (2011).
[34] E. Bermúdez-Ureña, C. Gonzalez-Ballestero, M. Geiselmann, R. Marty, I. P. Radko, T. Holmgaard, Y. Alaverdyan, E. Moreno, F. J. García-Vidal, S. I. Bozhevolnyi, and R. Quidant, Nat. Commun. **6**, 7883 (2015).
[35] M. Y. Shalaginov, V. V. Vorobyov, J. Liu, M. Ferrera, A. V. Akimov, A. Lagutchev, A. N. Smolyaninov, V. V. Klimov, J. Irudayaraj, A. V. Kildishev, A. Boltasseva, and V. M. Shalaev, Laser Photon. Rev. **9**, 120 (2015).
[36] E. M. Purcell, Phys. Rev. **69**, 681 (1946).
[37] S. A. Wolf, I. Rosenberg, R. Rapaport, and N. Bar-Gill, Phys. Rev. B **92**, 235410 (2015).
[38] T. M. Babinec, H. Fedder, J. Choy, I. Bulu, M. Doherty, P. Hemmer, J. Wrachtrup, and M. Loncar, in *Proceedings of CLEO: Science and Innonvations* (Optical Society of America, San Jose, CA, 2012), p. JW1I.6.
[39] A. Jarmola, Z. Bodrog, P. Kehayias, M. Markham, J. Hall, D. J. Twitchen, V. M. Acosta, A. Gali, and D. Budker, Phys. Rev. B **94**, 094108 (2016).
[40] J.-P. Tetienne, A. Lombard, D. A. Simpson, C. Ritchie, J. Lu, P. Mulvaney, and L. C. L. Hollenberg, Nano Lett. **16**, 326 (2016).
[41] J. M. Taylor, P. Cappellaro, L. Childress, L. Jiang, D. Budker, P. R. Hemmer, A. Yacoby, R. Walsworth, and M. D. Lukin, Nat. Phys. **4**, 810 (2008).
[42] S. Choi, J. Choi, R. Landig, G. Kucsko, H. Zhou, J. Isoya, F. Jelezko, S. Onoda, H. Sumiya, V. Khemani, C. von Keyserlingk, N. Y. Yao, E. Demler, and M. D. Lukin, Nature (London) **543**, 221 (2017).
[43] J. Choi, R. Landig, M. D. Lukin, D. Hopper, and L. Bassett (private communication).
[44] G. V. Naik, J. L. Schroeder, X. Ni, A. V. Kildishev, T. D. Sands, and A. Boltasseva, Opt. Mater. Express **2**, 478 (2012).
[45] S. A. Maier, *Plasmonics: Fundamentals and Applications* (Springer, Boston, 2007).
[46] See Supplemental Material at http://link.aps.org/supplemental/10.1103/PhysRevB.96.035146 for details of fabrication and characterization methods as well as modeling of lifetime shortening.
[47] L. Robledo, H. Bernien, T. Van Der Sar, and R. Hanson, New J. Phys. **13**, 025013 (2011).

[48] L. Robledo, L. Childress, H. Bernien, B. Hensen, P. F. A. Alkemade, and R. Hanson, Nature (London) **477**, 574 (2011).
[49] G. D. Fuchs, G. Burkard, P. V. Klimov, and D. D. Awschalom, Nat. Phys. **7**, 789 (2011).
[50] F. Jelezko, T. Gaebel, I. Popa, A. Gruber, and J. Wrachtrup, Phys. Rev. Lett. **92**, 076401 (2004).
[51] D. O'Connor and D. Phillips, *Time-Correlated Single Photon Counting* (Academic, London, 1984).
[52] F. A. Inam, T. Gaebel, C. Bradac, L. Stewart, M. J. Withford, J. M. Dawes, J. R. Rabeau, and M. J. Steel, New J. Phys. **13**, 073012 (2011).
[53] P. V. Ruijgrok, R. Wuest, A. A. Rebane, A. Renn, and V. Sandoghdar, Opt. Express **18**, 6360 (2010).
[54] A. Mohtashami and A. Femius Koenderink, New J. Phys. **15**, 043017 (2013).
[55] G. V. Naik, B. Saha, J. Liu, S. M. Saber, E. A. Stach, J. M. K. Irudayaraj, T. D. Sands, V. M. Shalaev, and A. Boltasseva, Proc. Natl. Acad. Sci. USA **111**, 7546 (2014).
[56] A. Gupta, L. Hacquebard, and L. Childress, J. Opt. Soc. Am. B **33**, B28 (2016).
[57] J. Wolters, M. Strauß, R. S. Schoenfeld, and O. Benson, Phys. Rev. A **88**, 020101 (2013).
[58] N. B. Manson, J. P. Harrison, and M. J. Sellars, Phys. Rev. B **74**, 104303 (2006).
[59] L. Li, E. H. Chen, J. Zheng, S. L. Mouradian, F. Dolde, T. Schröder, S. Karaveli, M. L. Markham, D. J. Twitchen, and D. Englund, Nano Lett. **15**, 1493 (2015).
[60] S. L. Mouradian, T. Schröder, C. B. Poitras, L. Li, J. Goldstein, E. H. Chen, M. Walsh, J. Cardenas, M. L. Markham, D. J. Twitchen, M. Lipson, and D. Englund, Phys. Rev. X **5**, 031009 (2015).